

IOWA STATE UNIVERSITY

Digital Repository

Agricultural and Biosystems Engineering
Publications

Agricultural and Biosystems Engineering

2012

E. coli Transport through Surface-Connected Biopores Identified from Smoke Injection Tests

Garey A. Fox
Oklahoma State University

Mikayla M. Marvin
Oklahoma State University

Jorge A. Guzman
United States Department of Agriculture

Chi K. Hoang
Iowa State University

Robert W. Malone
United States Department of Agriculture

See next page for additional authors

Follow this and additional works at: http://lib.dr.iastate.edu/abe_eng_pubs

 Part of the [Agriculture Commons](#), and the [Bioresource and Agricultural Engineering Commons](#)

The complete bibliographic information for this item can be found at http://lib.dr.iastate.edu/abe_eng_pubs/506. For information on how to cite this item, please visit <http://lib.dr.iastate.edu/howtocite.html>.

This Article is brought to you for free and open access by the Agricultural and Biosystems Engineering at Iowa State University Digital Repository. It has been accepted for inclusion in Agricultural and Biosystems Engineering Publications by an authorized administrator of Iowa State University Digital Repository. For more information, please contact digirep@iastate.edu.

Authors

Garey A. Fox, Mikayla M. Marvin, Jorge A. Guzman, Chi K. Hoang, Robert W. Malone, and Rameshwar S. Kanwar

E. COLI TRANSPORT THROUGH SURFACE-CONNECTED BIOPORES IDENTIFIED FROM SMOKE INJECTION TESTS

G. A. Fox, M. M. Marvin, J. A. Guzman, C. K. Hoang, R. W. Malone, R. S. Kanwar, M. J. Shipitalo

ABSTRACT. *Macropores are the primary mechanism by which fecal bacteria from surface-applied manure can be transported into subsurface drains or shallow groundwater bypassing the soil matrix. Limited research has been performed investigating fecal bacteria transport through specific macropores identified in the field. The objective of this research was to better understand how fecal bacteria, using Escherichia coli (E. coli) as an indicator organism, are transported through naturally occurring macropores and potential interactions between the macropore and soil matrix domains in the field under controlled experimental conditions. Direct injection/infiltration tests were conducted in two naturally occurring, surface-connected macropores (biopores) that penetrated to the subsurface drain depth, as identified by smoke tests. Data included total drain flow rate (baseflow rate and biopore flow rate), biopore inflow rate, and Rhodamine WT and E. coli concentrations in the drains. Analysis techniques included determining increases in subsurface drain flow rates due to the infiltration tests and percentage of the injected concentration reaching the subsurface drains after dilution with the drain baseflow. In the absence of data for mechanistic models, empirically based rational polynomial models were compared to the more commonly utilized lognormal distribution for modeling the load rate breakthrough curves. Load estimates were derived from integrated forms of these empirical functions, and percent reductions were calculated for Rhodamine WT and E. coli. Peak total drain flow rates increased nearly two-fold due to direct injection into the biopores. Less than 25% of the initial concentrations injected into the biopores reached the drain after dilution with the baseflow in the drain. Lognormal distributions best fit the Rhodamine WT load rate breakthrough curves ($R^2 = 0.99$ for both biopores) and the E. coli load rate data for one of the biopores ($R^2 = 0.98$). A rational fractional polynomial model that tailed off more slowly best fit the E. coli load rate data for the other biopore ($R^2 = 0.98$). Approximately one log reduction was estimated for E. coli loads due to interaction with the soil profile as water flowed through the tortuous path of the biopores; in other words, the soil surrounding the biopore filtered approximately 90% of the E. coli load that entered the biopore compared to approximately 75% for Rhodamine WT. Considering that applied animal manure can contain millions of bacteria per mL, high concentrations and loads are still possible in the subsurface drain flow if macropores are present.*

Keywords. *Biopore, E. coli, Fecal bacteria, Macropore flow, Subsurface drainage.*

Streamflow fecal microbial concentrations are commonly reported as an indicator of water quality degradation throughout the world (Gerba, 1996; Gale, 2001; Eyles et al., 2003; Haack et al., 2003;

Donner et al., 2006; Soller et al., 2010). Aged manures applied to agricultural fields as fertilizer are rich in fecal microbial populations in which the bacterium *Escherichia coli* (*E. coli*) is commonly used as an indicator of fecal contamination in soil and water (Gerba, 1996; Lapointe et al., 2009). The presence of the indicator bacteria is assumed to be associated with the presence of pathogenic microorganisms such as *E. coli* O:157:H7, *Salmonella*, and *Cryptosporidium parvum*.

Irrigation or rainfall occurring shortly after manure application can favor transport of fecal microorganisms to shallow aquifers and rivers (Soupir et al., 2006). Agricultural activities on poorly drained soils rely on subsurface drainage systems to increase efficiency. In fact, an estimated 2.4 to 3.6 million ha in Iowa are managed with subsurface drainage (Sugg, 2007). Transport of fecal bacteria such as *E. coli* to subsurface drains is commonly limited due to the soil filtration capacity (i.e., straining, sorption, and die-off). Fecal bacteria from manure applications are commonly particle-associated and filtered by the soil matrix, but rapidly transported to lower soil horizons through macropores (Mawdsley et al., 1996a, 1996b; Harter et al., 2000; Logan et al., 2001; McGehean and Vinten, 2003;

Submitted for review in April 2012 as manuscript number SW 9725; approved for publication by the Soil & Water Division of ASABE in October 2012.

The authors are **Garey A. Fox, ASABE Member**, Associate Professor and Orville L. and Helen L. Buchanan Chair, and **Mikayla M. Marvin**, Undergraduate Student and 2011-2012 Wentz/OSU Undergraduate Research Scholar, Department of Biosystems and Agricultural Engineering, Oklahoma State University, Stillwater, Oklahoma; **Jorge A. Guzman, ASABE Member**, Post-Doctoral Research Associate, USDA-ARS Grazinglands Research Laboratory, El Reno, Oklahoma; **Chi K. Hoang, ASABE Member**, Graduate Student, Department of Agriculture and Biosystems Engineering, Iowa State University, Ames, Iowa; **Robert W. Malone, ASABE Member**, Agricultural Engineer, USDA-ARS National Laboratory for Agriculture and the Environment, Ames, Iowa; **Ramesh S. Kanwar, ASABE Fellow**, C.F. Curtiss Distinguished Professor, Department of Agriculture and Biosystems Engineering, Iowa State University, Ames, Iowa; and **Martin J. Shipitalo**, Research Soil Scientist, USDA-ARS National Laboratory for Agriculture and the Environment, Ames, Iowa. **Corresponding author:** Garey A. Fox, Department of Biosystems and Agricultural Engineering, 120 Ag Hall, Oklahoma State University, Stillwater, OK 74078; phone: 405-744-8423; e-mail: garey.fox@okstate.edu.

Darnault et al., 2004; Bradford and Bettahar, 2005; Guzman et al., 2009; Fox et al., 2011).

Biopores are macropores created by roots, earthworms, and other biological activities (Shipitalo and Gibbs, 2000). Kemper et al. (1988) recognized the importance of biopores in infiltration and seepage from irrigation ditches. Biopores have also been suggested to be responsible for rapid peaks in concentrations observed in subsurface drainage following manure application (Dean and Foran, 1992; Joy et al., 1998; Shipitalo and Gibbs, 2000; Cook and Baker, 2001; Jamieson et al., 2002; Bicudo and Goyal, 2003; Fox et al., 2004, 2007; Guzman et al., 2009), especially when interconnected to subsurface drains (Akay and Fox, 2007; Akay et al., 2008). In the field, drain biopore interconnectivity has been investigated using smoke injected into drain lines (Shipitalo and Gibbs, 2005). Using smoke tests, Shipitalo and Gibbs (2005) characterized the biopore structure and surface connectivity. Akay and Fox (2007) and Akay et al. (2008) investigated the influences of macropore-drain connectivity on flow in the laboratory using artificial macropores. They demonstrated that open surface-connected and open surface-disconnected biopores were highly efficient flow pathways to subsurface drains. These observations were recently incorporated in the Root Zone Water Quality Model (RZWQM) as the express fraction (Fox et al., 2004, 2007) and the biopore concept (Guzman and Fox, 2012) to improve flow and fecal bacteria transport simulation at the subsurface drain when biopores are present.

Biopores are tortuous and can establish a dynamic interaction with the soil matrix surrounding the macropore. This interaction can result in retainment of solutes and bacteria along the macropore wall. Most flow and transport studies have been conducted under laboratory conditions with straight or slightly sinuous macropores (Guzman et al., 2009), but little research on contaminant transport has been conducted under field conditions. As a recent example, Meek et al. (2012) studied breakthrough data of a bromide tracer and *E. coli* from a single breakthrough event induced by irrigation after swine manure application in a subsurface-drained plot in Nashua, Iowa. They used regression modeling and suggested that rational polynomial functions were better suited than classical lognormal distributions for modeling the bromide and *E. coli* data from the plot-scale experiment, which markedly peaked and tailed off more slowly than predicted by the lognormal distribution.

The objective of this research was to quantify fecal bacteria transport using *E. coli* as an indicator organism through naturally occurring biopores in the field. Transport of *E. coli* was contrasted with a weakly sorbed dye, Rhodamine WT. Two open surface-connected biopores were identified in a field plot in Nashua, Iowa, using smoke tests and used to (1) quantify flow rates into the surface-connected biopores, (2) investigate *E. coli* and Rhodamine WT concentrations exiting the subsurface drain when injected directly into the biopore, (3) determine appropriate empirical functions for modeling load rate breakthrough data and verifying recently published research (Meek et al., 2012) on the use of rational polynomial functions, and (4) compare injected loads to those estimated in the outflow

using the empirical functions to determine retention/dilution of the injected *E. coli* and Rhodamine WT.

MATERIALS AND METHODOLOGY

FIELD EXPERIMENTS

Field tests were conducted in November 2009 at the Iowa State University Northeast Research Station near Nashua, Iowa (fig. 1). This site consists of thirty-six 0.4 ha subsurface-drained plots with various manure and fertilizer treatments (Bakhsh et al., 2002). Soils have seasonally high water tables and thus benefit from subsurface drainage with an average depth of 1.2 m and drain spacing of 28.5 m. Smoke tests were conducted on 12 November 2009 in plot 20 (fig. 1) following the procedures of Shipitalo and Gibbs (2000). In this plot, the soil was a Floyd sandy loam, fine-loamy, mixed, superactive, mesic aquic Pachic Hapludoll (63.6% sand, 32.2% silt, and 4.1% clay) with 3.9% soil organic matter and bulk density of 1.4 g cm^{-3} . Hydraulic conductivity of the soil matrix domain was approximately 0.7 cm h^{-1} (Guzman et al., 2009). No rainfall was recorded at the site for three weeks prior to the experiments.

A pump and blower were used to force smoke into the drain line at the sump (downstream end of the drainage line) in plot 20 (fig. 1). After the pump and blower were started, an ignited smoke cartridge (Superior Signal Co., Inc., Spotswood, N.J.) was inserted into the line. Macropores that emitted smoke were flagged using two different classifications: (1) diffuse smoke plumes within a larger soil area without an observable biopore at the surface were classified as surface-disconnected biopores and hypothesized to be buried or disconnected macropores to the drain, and (2) concentrated smoke plumes emanating from visible biopores were classified as open surface-connected biopores and presumed to penetrate the soil profile and connect to the subsurface drain (drain-macropore interconnection) (fig. 2).

Two 1 to 2 cm diameter, open surface-connected biopores were identified for direct injection tests (fig. 1). The injection tests used a Mariotte-type infiltrometer with a to-

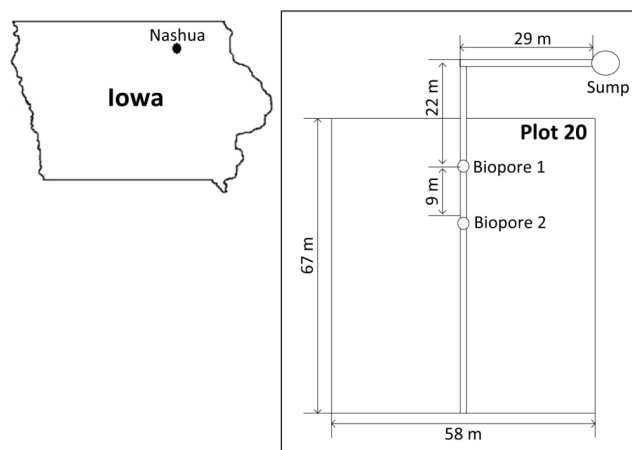


Figure 1. Location of the Iowa State University Northeast Research Station near Nashua, Iowa, and diagram of plot 20.



Figure 2. (a) Flagged macropores where smoke was visible on the surface, (b) the smoke bomb that was placed into sump, and (c) smoke and earthworm at the surface during a smoke test, indicating drain-macropore interconnectivity.

tal volume of 13 L to maintain a constant head of water within a small funnel, as performed by Shipitalo et al. (2004) and shown in figure 3. The volume of the initial water level in the infiltrometer and the infiltration rate controlled the duration of the injection experiment. Two infiltration tests were performed in each biopore: the first one with water containing Rhodamine WT followed by one with diluted liquid swine manure. Note that the swine ma-

nure infiltration test was conducted after the discharge flow at the outlet of the drain pipe returned to pre-injection rates. Water levels in the infiltrometer were recorded every minute until the water was exhausted. The rate at which the solution entered the biopore was used to quantify the steady-state infiltration rate into the biopores, a function of the moisture content of the soil surrounding the biopore. Infiltration experiments lasted approximately 15 to 20 min.

Drain flow rates were monitored in the sump over time using an automated pump system that turned on when a specific height of water in the sump was achieved. Rhodamine WT and *E. coli* concentrations were monitored in the drain flow at the sump for approximately 90 min after initiation of the infiltration experiments. The outlet of the drain pipe in the sump (i.e., sample collection location) was above the sump water level. A 100 mL sample bottle was filled using a PVC pipe manually lowered into the sump. The pipe had a 45° elbow at the bottom which housed the sample bottle. No specific time sampling scheme was used. Samples were collected throughout the concentration breakthrough curves, visually determined from the presence of Rhodamine WT dye in the outflow. *E. coli* concentrations were quantified using IDEXX Colilert reagent and Quanti-Tray 2000 (IDEXX, Westbrook, Maine), a U.S. EPA-approved method for *E. coli* quantification, based on the most probable number (MPN) test (Guzman et al., 2009; Garbrecht et al., 2009; Guzman et al., 2010, 2012). The method provides counts from one to approximately 2,419 per 100 mL (IDEXX, Westbrook, Maine). Rhodamine WT concentrations were measured with a Trilogy laboratory fluorometer (Turner Designs, Inc., Sunnyvale, Cal.) that had a minimum detection limit of $10 \mu\text{g L}^{-1}$. Initial infiltrometer concentrations of Rhodamine WT and *E. coli* injected into the biopore were quantified and considered to remain constant throughout the experiment: 7,798 and $15,798 \mu\text{g L}^{-1}$ for Rhodamine WT and 12,997

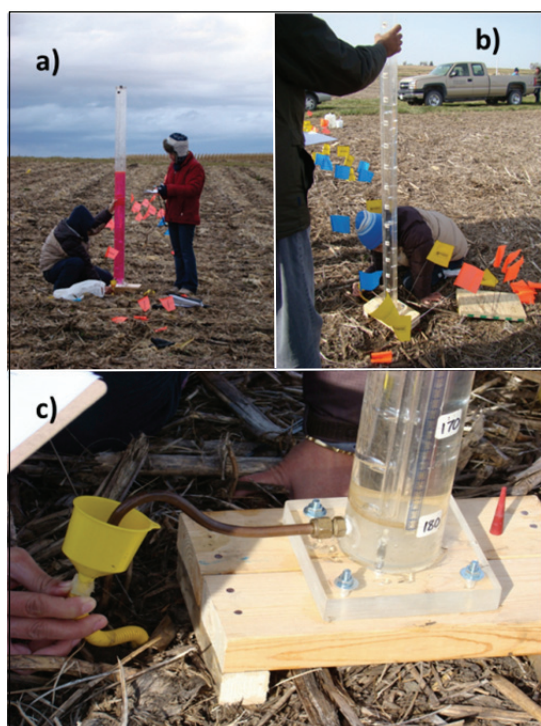


Figure 3. (a) Rhodamine WT solution in a Mariotte-type constant-head infiltrometer used for the infiltration experiments into surface-connected biopores, and (b and c) inserting the funnel tube into a flagged biopore.

and 51,720 MPN per 100 mL for *E. coli* in biopores 1 and 2, respectively. Note that the variability in the inflow *E. coli* concentrations was due to adding a specified volume of diluted swine manure to the infiltrometer rather than a measured mass or number of bacteria. The concentration of *E. coli* in diluted liquid swine manure can be variable (Guzman et al., 2012).

CALCULATING INFLOW AND OUTFLOW LOADS

Data for the biopore field tests were analyzed in order to determine steady-state infiltration rates and the Rhodamine WT and *E. coli* loads reaching the drain outlet after direct injection. The inflow load injected into the biopore (L_{IN} , μg for Rhodamine WT and MPN for *E. coli*) was calculated using the following equations (eq. 1a for Rhodamine WT and eq. 1b for *E. coli*) since the infiltration rate quickly became steady after the injection started:

$$L_{IN} = \frac{Q_{IN} C_0 t_d}{1000} \quad (1a)$$

$$L_{IN} = Q_{IN} C_0 t_d \quad (1b)$$

where Q_{IN} is the steady-state water flow rate into the biopore derived from the infiltrometer (mL s^{-1}), C_0 is the constant concentration of Rhodamine WT ($\mu\text{g L}^{-1}$) or *E. coli* (MPN per 100 mL) in the inflow solution, t_d is the time duration of the infiltration experiment (s), and the factor of 1000 in equation 1a is a conversion between mL and L.

In order to solve for the load out of the drain (L_{OUT}), the flow rates measured at the sump were needed. Flow hydrographs were observed in the drain flow at the sump due to increases in flow from the injection beyond the drain baseflow rate. The sumps only measured flow rates periodically based on a volume basis (i.e., the sumps turned on when the water level in the sump reached a specific height), resulting in a limited number of data points. Therefore, the flow rates entering the sump (total drain flow rate, Q) were plotted versus time, and polynomial trend lines were fit to these data. The use of more sophisticated regression equations was precluded by the relatively few data points for each experiment.

The equations for the trend lines were then used to estimate the total drain flow rates (Q_i) at the times corresponding to the outflow (i.e., drain flow) concentration (C_i) measurement times (t_i). Outflow concentrations from the drain were diluted as a function of the volume of water entering the drain pipe along the length of the pipe and as a function of the travel time between the injection and observation points. Note that computations were based on total load (mass balance), and samples were taken until concentrations fell near the detection level ($10 \mu\text{g L}^{-1}$ for Rhodamine WT and 1 MPN per 100 mL for *E. coli*). These data were then used to calculate the load rate for each time increment L_i in units of $\mu\text{g s}^{-1}$ for Rhodamine WT (eq. 2a) and MPN s^{-1} for *E. coli* (eq. 2b):

$$L_i = \frac{Q_i C_i}{1000} \quad (2a)$$

$$L_i = Q_i C_i \quad (2b)$$

MODELING LOAD RATE BREAKTHROUGH CURVES

In the absence of data for simulating the transport process using mechanistic models, such as characteristics of the macropore (diameter, length, sinuosity, and connectedness to the drain), *E. coli* (sorption and die-off coefficients), and the soil (hydrodynamic dispersion coefficient), empirically based rational polynomial models (RPM) were compared to the more commonly utilized lognormal distribution for modeling the Rhodamine WT and *E. coli* load rate breakthrough curves. This research was aimed at verifying the consistency of the conclusions reported by Meek et al. (2012) and therefore utilized the same four RPMs:

$$L(t) = \frac{t}{a + bt + ct^2} \quad (3)$$

$$L(t) = \frac{1}{a + b\sqrt{t} + ct} \quad (4)$$

$$L(t) = \frac{\sqrt{t}}{a + b\sqrt{t} + ct} \quad (5)$$

$$L(t) = \frac{t}{a + b\sqrt{t} + ct} \quad (6)$$

where a , b , and c are fitted model parameters, $L(t)$ is the measured load rate ($\mu\text{g s}^{-1}$ for Rhodamine WT and MPN s^{-1} for *E. coli*), and t is time (s). As noted by Meek et al. (2012), equation 6 is commonly referred to as the Gunary model. The lognormal distribution is given by the following equation:

$$L(t) = \frac{a}{\sqrt{2\pi}tb} \exp \left\{ -\frac{\left[\log \left(\frac{t}{c} \right) \right]^2}{2b^2} \right\} \quad (7)$$

Parameter estimation was performed using a nonlinear regression scheme in SigmaStat (v11, Systat Software, Inc., San Jose, Cal.), which uses a Marquardt-Levenberg algorithm (Press et al., 1986). Initial parameter values were derived using the transformed independent variables reported by Meek et al. (2012). Parameter values were derived along with a standard error. Model performance was based on the coefficient of determination (R^2), the adjusted R^2 , and the standard error, all reported by SigmaStat (v11).

Equations 3 through 7 were then integrated over the experimental duration to derive an estimate of the total load (L_{OUT}) for each RPM and the lognormal distribution. The L_{OUT} was also estimated from the experimental data using a numerical integration technique and compared to the load estimates derived with the empirical functions:

$$L_{OUT} = \int Q C dt = \sum_{i=1}^n Q_i C_i \Delta t \quad (8)$$

where n is the number of data points, and Δt is the time interval. Load values from both the integrated mathematical functions and the experimental data were used to calculate percent reductions for Rhodamine WT and *E. coli* for each biopore experiment:

$$\% \text{ Reduction} = \left(\frac{L_{IN} - L_{OUT}}{L_{IN}} \right) 100\% \quad (9)$$

RESULTS AND DISCUSSION

SMOKE TESTS

The macropores identified during the smoke tests were primarily biopores created by anecic, or deep-burrowing, species of earthworms (fig. 2). The number of macropores emitting smoke during this experiment is shown in figure 4. The total number of macropores was 77, with an approximate density of one per m along the drain line. Of these 77 macropores, about 26 produced concentrated smoke plumes and were presumed to be directly connected to the drain line. Interestingly, smoke tests on the same plot conducted throughout a two-year period demonstrated a much greater number of macropores present in the late fall (usually on the order of 1 to 2 macropores per m) compared to the early spring just after the frozen soil thawed. This was explained as a function of earthworm activity following a dormant stage during winter.

DRAIN FLOW RATES

Steady-state infiltration rates in biopore 1 were 11.0 mL s^{-1} for the Rhodamine WT injection experiment and 9.1 mL s^{-1} for the *E. coli* injection experiment. Corresponding values for biopore 2 were 17.1 and 11.0 mL s^{-1} (fig. 5). The decrease in steady-state infiltration rate was hypothesized to be due to a wetted soil matrix during the second direct injection when using the diluted swine manure. In addition, the diluted manure contained particulate matter that may have clogged some of the smaller pores, thereby reducing the infiltration rates. The slower infiltration rates early in the manure injection into biopore 2 were potentially due to settled solids from the manure clogging the funnel flow. Note that for macropore 2 (fig. 5b) the infiltration rate was

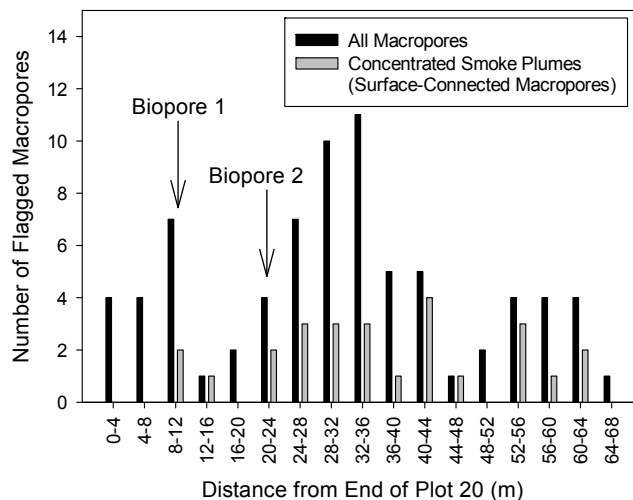


Figure 4. Number of flagged macropores relative to distance along the length of the subsurface drain. Length is measured from the downstream end of the plot. Also indicated is the number of concentrated smoke plume macropores (surface-connected), hypothesized to penetrate to the subsurface drain.

derived based on the average trend line through all the data, including data when the infiltration rate slowed approximately 2 to 5 min into the injection. Using only the latter half of the data resulted in a much more comparable infiltration rate to that measured during the first Rhodamine WT injection for that macropore. These biopores had much higher flow rates per unit area compared to the surrounding soil matrix and most likely serve as the primary flow pathway into the subsurface drains during and immediately after a rainfall.

Direct injection into a biopore increased the drain flow rates measured at the sump by approximately two-fold (fig. 6); flow rates increased from approximately 5 mL s^{-1} at the beginning and peaked at approximately 10 to 12 mL s^{-1} . Faster breakthrough times (i.e., increases in drain flow rates and less time to reach peak drain flow rates at the sump) were observed for the manure injection than for the Rhodamine WT injection (fig. 6). This occurred because the Rhodamine WT injections were performed first, when the soil profile around the biopore was drier. This resulted in more water from the Rhodamine WT injection diffusing

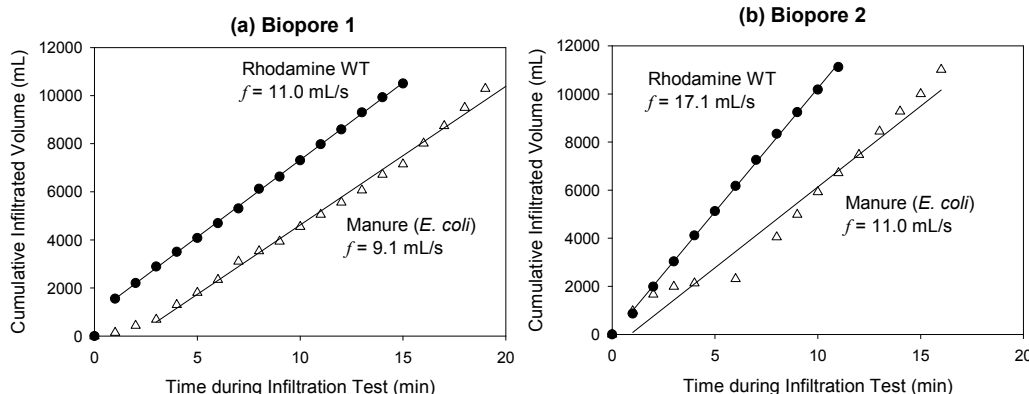


Figure 5. Cumulative infiltrated volume versus time for (a) biopore 1 and (b) biopore 2. The slopes were used to obtain steady-state infiltration rates (f) for each experiment.

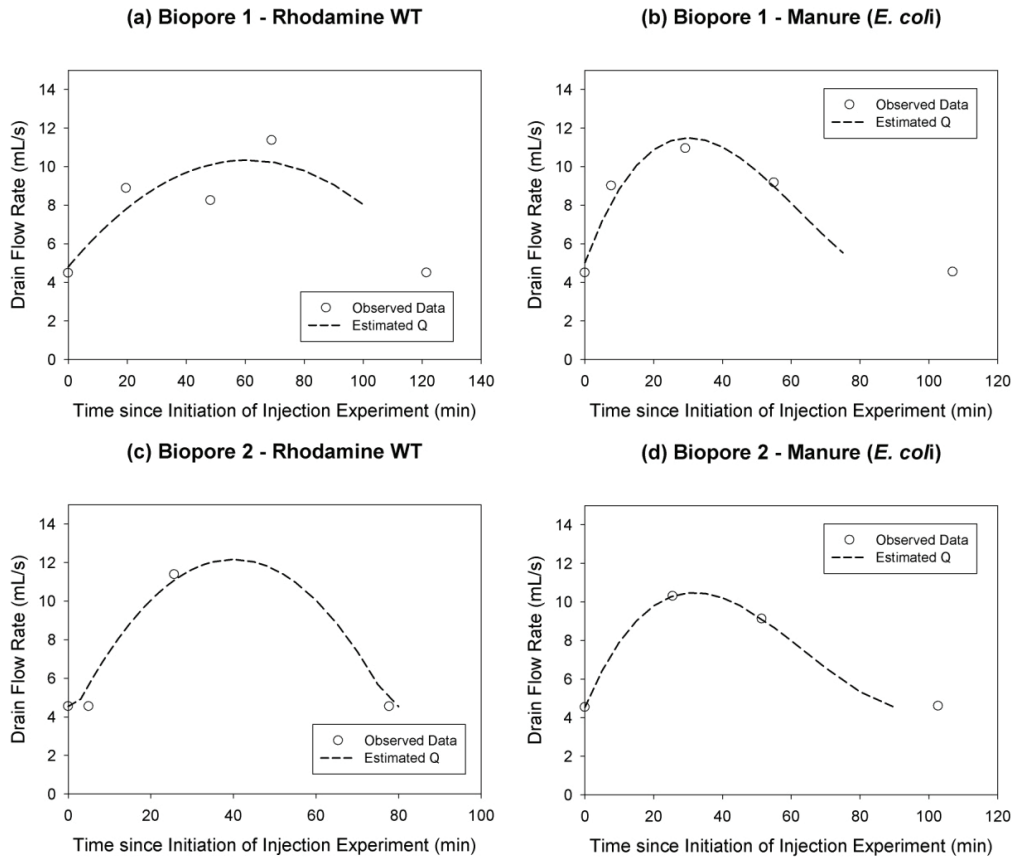


Figure 6. Drain flow rates for each of the direct injection experiments. Symbols (circles) are the observed drain flow rates measured in the sump. Dashed lines are estimated drain flow rates during the time period in which concentrations were measured in the sump.

into the soil profile surrounding the biopore, and thus a more elongated curve (fig. 6). More water was measured in the sump than injected into the biopore; therefore, a water mass balance was not possible for these experiments. Potentially, this discrepancy was due to the measurement technique of drain flow rates; some water was most likely stored in the sump prior to beginning the experiment. Water may have also been released from storage in the soil due to the infiltration around the biopore. More precise drainage flow measurements are needed in future experiments.

RHODAMINE WT AND *E. COLI* CONCENTRATIONS

Peak Rhodamine WT concentrations in the outflow were 15% to 25% of the initial inflow concentrations (C_0) in the infiltrometer (fig. 7). Corresponding values for peak *E. coli* concentrations were 5% to 15%. These concentrations were diluted by the baseflow in the drain prior to the experiment. Guzman et al. (2009) reported soil column experiments on artificial, straight macropores with this same soil. Peak *E. coli* concentrations were 4% of the inflow concentration for transport in macropores that were surface-connected but did not extend to the drain depth in the soil profile (55 cm

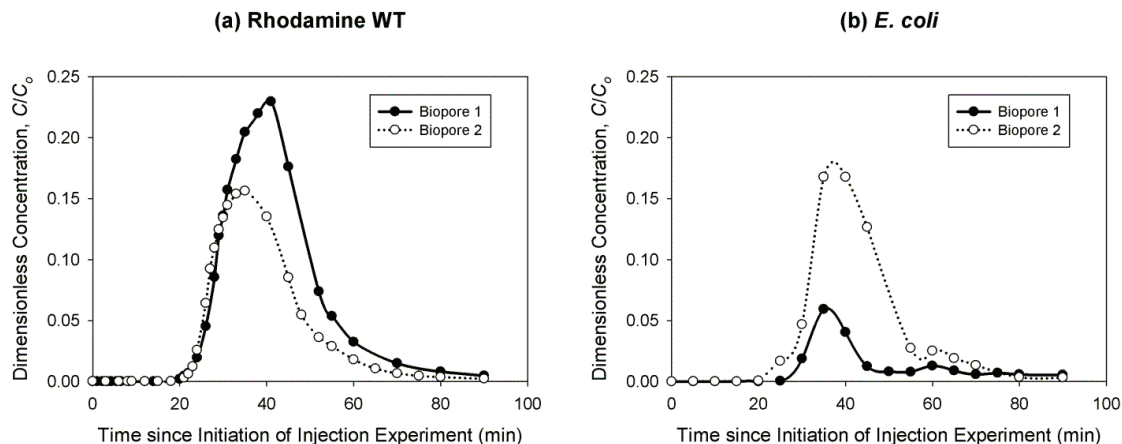


Figure 7. Concentrations of (a) Rhodamine WT and (b) *E. coli* in the drain flow (measured at the sump in fig. 1) relative to the initial concentration (C_0) injected into the biopore.

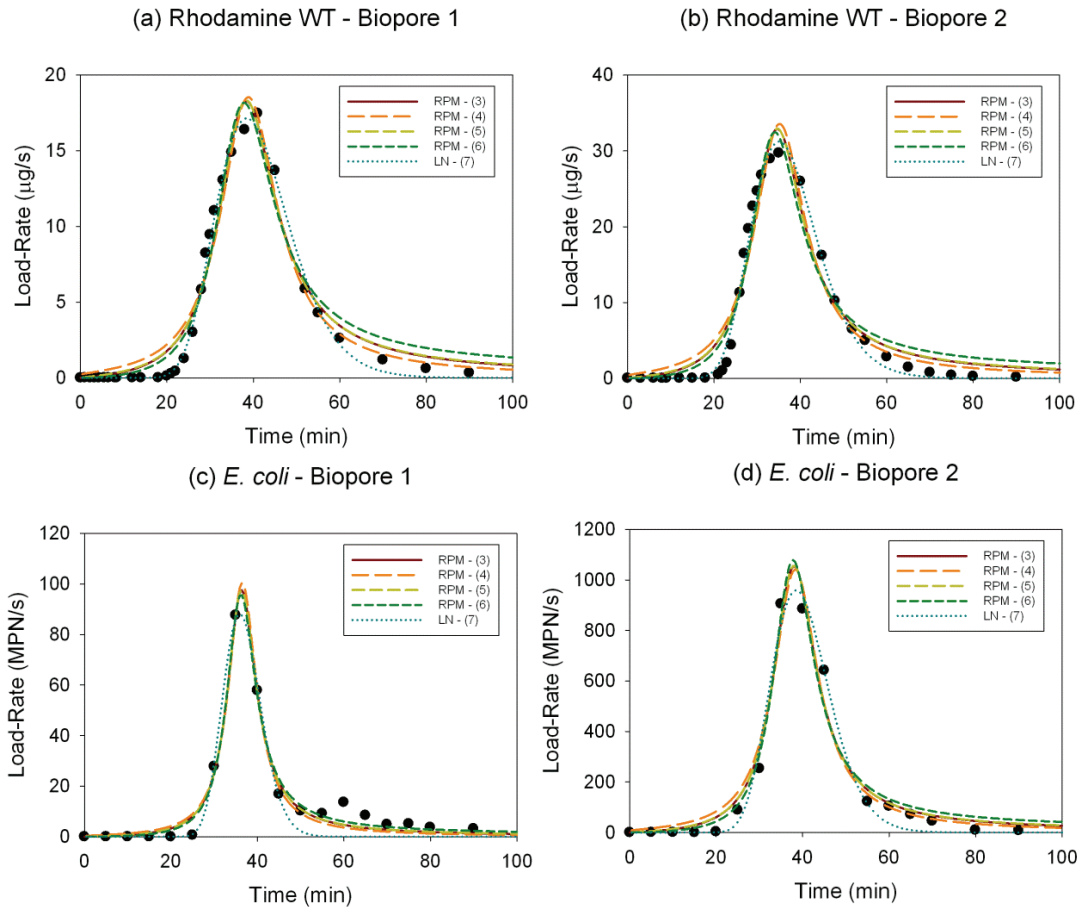


Figure 8. Drainage load rate breakthrough curves for Rhodamine WT and *E. coli* directly injected into two directly connected biopores. Measurements (symbols) are fit to the rational polynomial models (eqs. 3 to 6) and the lognormal distribution (LN, eq. 7) using SigmaStat (v11).

instead of 70 cm) and that were not diluted by a baseflow component. Therefore, these concentrations measured in the drain outflow were somewhat comparable to laboratory experiments. Even though the concentration reductions were substantial, when considering microorganisms from manure sources applied to the field in large amounts, the total number of bacteria that can reach the subsurface drain can be quite high in the presence of macropores. Note the differences in breakthrough times and relative concentrations of Rhodamine WT and *E. coli* between the two biopores. The inconsistent relationships may be due to differences in biopore lengths, sinuosity, and/or biopore-drain connectedness, which influence soil matrix-macropore interaction. Such hypotheses were not able to be investigated further in these experiments.

LOAD RATE BREAKTHROUGH CURVES

The lognormal distribution was the best fit to the Rhodamine WT breakthrough curves for both biopores; the Gunary model, as shown in equation 6, was the best fit for the *E. coli* breakthrough curves for biopore 1, while the lognormal distribution was the best fit for biopore 2 (fig. 8 and table 1). Note the closeness of the R^2 , adjusted R^2 , and standard errors for the lognormal distribution and Gunary model for *E. coli* transport through biopore 2. Meek et al. (2012) reported that specific RPMs performed better than the lognormal distribution for their single-event, plot-scale

data, where they observed extended tails on the breakthrough curves for both bromide and *E. coli*. In this research, the slow tailing effect was more pronounced for the stronger sorbing *E. coli* as compared to the slightly sorbing Rhodamine WT (Guzman et al., 2012). The advantage of the lognormal function was its ability to match observations near the peak for these experimental data (fig. 8). The more apparent tailing effect in the plot-scale study reported by Meek et al. (2012) may be due to a distribution of macropores with varying connectivity to subsurface drainage contributing to bromide and *E. coli* transport, whereas our results are from only one macropore at a time. This suggests the need for further field-scale research as opposed to laboratory-scale macropore experiments.

In both biopores, a greater percent load reduction was observed for *E. coli* than for Rhodamine WT (table 2). Equivalent to the fit for the load rate curves, the integrated logarithmic function most closely matched the integrated experimental data for Rhodamine WT for both biopores and *E. coli* for biopore 2. It was interesting to observe an approximate one log scale (90%) reduction in *E. coli* loads even when injected into a directly connected biopore. This reduction was not proportional to the sorption capability of Rhodamine WT or *E. coli*. In fact, previous studies have indicated that the sorption potential of *E. coli* to this soil (Guzman et al., 2012) is much greater than the sorption potential of Rhodamine WT. The most likely explanation

Table 1. Load rate breakthrough curve regression results for Rhodamine WT and *E. coli* when using the rational polynomial models (RPMs, eqs. 3 to 6) and the lognormal model (eq. 7) using SigmaStat (v11).^[a]

| | | Equation | R ² | Adj. R ² | SE _{estimate} | a ±SE _{parameter} | b ±SE _{parameter} | c ±SE _{parameter} |
|----------------------------|-----------|----------|----------------|---------------------|------------------------|----------------------------|----------------------------|----------------------------|
| Rhodamine WT, Biopore 1 | RPMs | 3 | 0.96 | 0.96 | 1.12 | 44.52 ±4.15 | -2.26 ±0.22 | 0.03 ±0.00 |
| | | 4 | 0.95 | 0.95 | 1.27 | 5.04 ±0.52 | -1.60 ±0.17 | 0.13 ±0.01 |
| | | 5 | 0.96 | 0.96 | 1.13 | 29.04 ±2.76 | -9.32 ±0.90 | 0.76 ±0.07 |
| | | 6 | 0.96 | 0.96 | 1.14 | 175.85 ±16.92 | -57.16 ±5.55 | 4.70 ±0.46 |
| | Lognormal | 7 | 0.99 | 0.99 | 0.45 | 161.41 ±2.66 | 0.10 ±0.00 | 40.39 ±0.17 |
| Rhodamine WT, Biopore 2 | RPMs | 3 | 0.95 | 0.94 | 2.57 | 23.06 ±2.56 | -1.30 ±0.15 | 0.02 ±0.00 |
| | | 4 | 0.93 | 0.92 | 2.87 | 2.79 ±0.34 | -0.93 ±0.12 | 0.08 ±0.01 |
| | | 5 | 0.94 | 0.94 | 2.60 | 15.83 ±1.78 | -5.35 ±0.61 | 0.46 ±0.05 |
| | | 6 | 0.95 | 0.94 | 2.53 | 94.43 ±10.44 | -32.36 ±3.61 | 2.80 ±0.31 |
| | Lognormal | 7 | 0.99 | 0.99 | 1.15 | 262.83 ±5.66 | 0.09 ±0.00 | 36.74 ±0.19 |
| <i>E. coli</i> , Biopore 1 | RPMs | 3 | 0.98 | 0.97 | 3.90 | 28.82 ±4.01 | -1.58 ±0.22 | 0.02 ±0.00 |
| | | 4 | 0.97 | 0.96 | 4.40 | 3.38 ±0.54 | -1.11 ±0.18 | 0.09 ±0.01 |
| | | 5 | 0.98 | 0.97 | 3.89 | 19.21 ±2.63 | -6.36 ±0.86 | 0.53 ±0.07 |
| | | 6 | 0.98 | 0.98 | 3.51 | 113.22 ±13.61 | -37.64 ±4.46 | 3.14 ±0.36 |
| | Lognormal | 7 | 0.95 | 0.94 | 5.87 | 423.34 ±27.59 | 0.05 ±0.00 | 36.49 ±0.34 |
| <i>E. coli</i> , Biopore 2 | RPMs | 3 | 0.97 | 0.96 | 60.21 | 1.37 ±0.21 | -0.07 ±0.01 | 9.00e-4 ±1.00e-4 |
| | | 4 | 0.96 | 0.95 | 68.59 | 0.14 ±0.02 | -0.05 ±0.01 | 3.70e-3 ±6.0e-4 |
| | | 5 | 0.97 | 0.96 | 60.77 | 0.90 ±0.14 | -0.29 ±0.04 | 0.02 ±3.60e-3 |
| | | 6 | 0.97 | 0.97 | 58.71 | 5.87 ±0.87 | -1.91 ±0.28 | 0.16 ±0.02 |
| | Lognormal | 7 | 0.98 | 0.98 | 49.28 | 7051.72 ±341.15 | 0.08 ±0.00 | 39.68 ±0.39 |

^[a] SE_{estimate} = standard error of the estimate, and SE_{parameter} = standard error of the parameter.

Table 2. Inflow and outflow Rhodamine WT and *E. coli* loads (percent reductions in outflow loads shown in parentheses). Outflow loads were calculated using integrated rational polynomial models (RPMs), the integrated logarithmic function, and a numerical integration of the experimental data.

| | | Rhodamine WT (mg) | | <i>E. coli</i> (MPN) | |
|--------------|-----------------------------------|-------------------|-----------|------------------------------|------------------------------|
| | | Biopore 1 | Biopore 2 | Biopore 1 | Biopore 2 |
| Inflow load | | 77 | 179 | 1.35 × 10 ⁶ | 5.81 × 10 ⁶ |
| Outflow load | RPM, equation 3 | 26 (66%) | 43 (76%) | 7.29 × 10 ⁴ (95%) | 1.14 × 10 ⁶ (80%) |
| | RPM, equation 4 | 25 (67%) | 42 (76%) | 7.14 × 10 ⁴ (95%) | 1.13 × 10 ⁶ (81%) |
| | RPM, equation 5 | 26 (66%) | 43 (76%) | 7.31 × 10 ⁴ (95%) | 1.15 × 10 ⁶ (80%) |
| | RPM, equation 6 | 27 (65%) | 44 (76%) | 7.55 × 10 ⁴ (94%) | 1.17 × 10 ⁶ (80%) |
| | Lognormal function | 22 (71%) | 36 (81%) | 5.85 × 10 ⁴ (94%) | 9.83 × 10 ⁵ (83%) |
| | Integrated from experimental data | 21 (73%) | 34 (81%) | 7.56 × 10 ⁴ (94%) | 9.83 × 10 ⁵ (83%) |

for the greater reduction in *E. coli* is that Rhodamine WT was completely dissolved in water, while *E. coli* from manure application were generally attached to suspended organic colloids, causing the bacteria to be removed more easily in sinuous areas of the macropore (Guzman et al., 2009). Another unknown contribution to *E. coli* removal could have been settling of particle-associated *E. coli* in the subsurface drain flow and/or sorption to biofilms on the subsurface drain walls. Particle-associated *E. coli* were subject to settling under low velocity conditions. The second biopore had more similar reduction rates than the first between *E. coli* and Rhodamine WT injections; hypothetically, this could be due to the first biopore being more sinuous than the second, or due to differences in biopore-drain connectedness. However, this could not be determined in this experiment, as the plot needed to stay intact for other research projects.

CONCLUSIONS

Research on *E. coli* transport through soil macropores is important for a better understanding of water quality issues surrounding agricultural practices in areas with subsurface drainage systems or shallow water tables. This research showed that injection into a single biopore increased the flow rate in the drain two-fold. Larger numbers of contrib-

uting macropores could increase drain flow substantially. The concentrations of *E. coli* and Rhodamine WT at the drain were less than 25% of the initial concentrations injected into the biopore for all experiments due to the interaction of the soil and macropore domains, dilution with the drainage baseflow, and settling of particle-associated bacteria. This number seems small, but when manure with a high concentration of *E. coli* is applied to the field, the number of bacteria entering the drain can still be large enough to cause water quality degradation. Both lognormal and rational polynomial models fit the Rhodamine WT and *E. coli* load rate breakthrough curves and outflow loads. Lognormal functions with less apparent tailing than the rational polynomial models may be better suited when modeling individual macropores but less appropriate for field-scale studies with a range of macropore-drainage connectivity pathways. The load reduction for *E. coli* when transported through an individual biopore was approximately 90% but varied for each biopore. Further experimentation should be performed to determine the influence of scale in modeling macropore flow and transport, the effects of the shapes of the macropores on load concentrations out of drains, the partitioning of *E. coli* to particles in subsurface drainage waters, and how management practices can be altered to reduce water degradation from *E. coli* transport through macropores.

ACKNOWLEDGEMENTS

The authors would like to acknowledge funding support through the 2011-2012 Lew Wentz Undergraduate Research Scholars Program at Oklahoma State University and a 2007-2011 USDA-CSREES National Research Initiative Grant (Award No. 2007-35102-18242).

REFERENCES

- Akay, O., and G. A. Fox. 2007. Experimental investigation of direct connectivity between macropores and subsurface drains during infiltration. *SSSA J.* 71(5): 1600-1606.
- Akay, O., G. A. Fox, and J. Simunek. 2008. Numerical simulation of flow dynamics during macropore-subsurface drain interaction using HYDRUS. *Vadose Zone J.* 7(3): 909-918.
- Bakhsh, A., R. S. Kanwar, T. B. Bailey, C. A. Cambardella, D. L. Karlen, and T. S. Colvin. 2002. Cropping system effects on NO₃-N loss with subsurface drainage water. *Trans. ASAE* 45(6): 1789-1797.
- Bicudo, J. R., and S. M. Goyal. 2003. Pathogens and manure management systems: A review. *Environ. Tech.* 24(1): 115-130.
- Bradford, S. A., and M. Bettahar. 2005. Straining, attachment, and detachment of *Cryptosporidium* oocysts in saturated porous media. *J. Environ. Qual.* 34(2): 469-478.
- Cook, M. J., and J. L. Baker. 2001. Bacteria and nutrient transport to tile lines shortly after application of large volumes of liquid swine manure. *Trans. ASAE* 44(3): 495-503.
- Darnault, C. J. G., T. S. Steenhuis, P. Garnier, Y. J. Kim, M. B. Jenkins, W. C. Ghiorse, P. C. Baveye, and J. Y. Parlange. 2004. Preferential flow and transport of *Cryptosporidium parvum* oocysts through the vadose zone: Experiments and modeling. *Vadose Zone J.* 3(1): 262-270.
- Dean, D. M., and M. E. Foran. 1992. The effect of farm liquid waste application on tile drainage. *J. Soil Water Cons.* 47(5): 368-369.
- Dorner, S. M., W. B. Anderson, R. M. Slawson, N. Kouwen, and P. M. Huck. 2006. Hydrologic modeling of pathogen fate and transport. *Environ. Sci. Tech.* 40(15): 4746-4753.
- Eyles, R., D. Niyogi, C. Townsend, G. Benwell, and P. Weinstein. 2003. Spatial and temporal patterns of *Campylobacter* contamination underlying public health risk in the Taieri River, New Zealand. *J. Environ. Qual.* 32(5): 1820-1828.
- Fox, G. A., R. Malone, G. J. Sabbagh, and K. Rojas. 2004. Interrelationship of macropore flow and subsurface drainage: Influence on conservative tracer and pesticide transport. *J. Environ. Qual.* 33(6): 2281-2289.
- Fox, G. A., G. J. Sabbagh, R. W. Malone, and K. Rojas. 2007. Modeling parent and metabolite fate and transport in subsurface-drained fields with directly connected macropores. *J. American Water Resour. Assoc.* 43(6): 1359-1372.
- Fox, G. A., E. M. Matlock, J. A. Guzman, D. Sahoo, and K. B. Stunkel. 2011. *Escherichia coli* load reduction from runoff by vegetative filter strips: A laboratory-scale study. *J. Environ. Qual.* 40(3): 980-988.
- Gale, P. 2001. Developments in microbiological risk assessment for drinking water. *J. Appl. Microbiol.* 91(2): 191-205.
- Garbrecht, K., G. A. Fox, J. A. Guzman, and D. Alexander. 2009. *E. coli* transport through soil columns: Implications for bioretention cell removal efficiency. *Trans. ASABE* 52(2): 481-486.
- Gerba, C. P. 1996. Pathogens in the environment. In *Pollution Science*, 279-300. I. L. Pepper, C. P. Gerba, and M. L. Brusseau, eds. San Diego, Cal.: Academic Press.
- Guzman, J. A., and G. A. Fox. 2012. Implementation of biopore and fecal bacteria fate and transport routines into the Root Zone Water Quality Model (RZWQM). *Trans. ASABE* 55(1): 74-83.
- Guzman, J. A., G. A. Fox, R. W. Malone, and R. Kanwar. 2009. *Escherichia coli* transport from surface-applied manure to subsurface drains through artificial biopores. *J. Environ. Qual.* 38(6): 2412-2421.
- Guzman, J. A., G. A. Fox, and J. Payne. 2010. Surface runoff transport of *Escherichia coli* after poultry litter application on pastureland. *Trans. ASABE* 53(3): 779-786.
- Guzman, J. A., G. A. Fox, and C. Penn. 2012. Sorption of *Escherichia coli* in agricultural soils influenced by swine manure constituents. *Trans. ASABE* 55(1): 61-72.
- Haack, S., L. R. Fogarty, and C. Wright. 2003. *Escherichia coli* and *Enterococci* at beaches in the Grand Traverse Bay, Lake Michigan: Sources, characteristics, and environmental pathways. *Environ. Sci. Tech.* 37(15): 3275-3282.
- Harter, T., S. Wagner, and E. R. Atwill. 2000. Colloid transport and filtration of *Cryptosporidium parvum* in sandy soils and aquifer sediments. *Environ. Sci. Tech.* 34(1): 62-70.
- Jamieson, R. C., R. J. Gordon, K. E. Sharples, G. W. Stratton, and A. Madani. 2002. Movement and persistence of fecal bacteria in agricultural soils and subsurface drainage water: A review. *Canadian Biosystems Eng.* 44: 1.1-1.9.
- Joy, D. M., H. Lee, C. M. Reaume, H. R. Whiteley, and S. Zelin. 1998. Microbial contamination of subsurface tile drainage water from field applications of liquid manure. *Canadian Agric. Eng.* 40(3): 153-160.
- Kemper, W. D., P. Jolley, and R. C. Rosenau. 1988. Soil management to prevent earthworms from riddling irrigation ditch banks. *Irrig. Sci.* 9(2): 79-87.
- Lapointe, T. K., P. M. O'Conner, and A. G. Buret. 2009. The role of epithelial malfunction in the pathogenesis of enteropathogenic *E. coli*-induced diarrhea. *Lab. Invest.* 89(9): 964-970.
- Logan, A. J., T. K. Stevik, R. L. Siegrist, and R. M. Ronn. 2001. Transport and fate of *Cryptosporidium parvum* oocysts in intermittent sand filters. *Water Res.* 35(18): 4359-4369.
- Mawdsley, J. L., A. E. Brooks, R. J. Merry, and B. F. Pain. 1996a. Movement of the protozoan pathogen *Cryptosporidium parvum* through three contrasting soil types. *Biol. Fertil. Soils* 21(1-2): 30-36.
- Mawdsley, J. L., A. E. Brooks, R. J. Merry, and B. F. Pain. 1996b. Use of a novel soil tilting table apparatus to demonstrate the horizontal and vertical movement of the protozoan pathogen *Cryptosporidium parvum* in soil. *Biol. Fertil. Soils* 23(2): 215-220.
- McGeachan, M. B., and A. J. A. Vinten. 2003. Simulation of transport through soil of *E. coli* derived from livestock slurry using the MACRO model. *Soil Use Mgmt.* 19(4): 321-330.
- Meek, D. W., C. Hoang, R. W. Malone, R. S. Kanwar, G. A. Fox, J. A. Guzman, M. J. Shipitalo. 2012. Technical note: Rational polynomial functions for modeling *E. coli* and bromide breakthrough. *Trans. ASABE* 55(5): 1821-1826.
- Press, W. H., B. P. Flannery, S. A. Teukolsky, and W. T. Vetterling. 1986. *Numerical Recipes*. Cambridge, U.K.: Cambridge University Press.
- Shipitalo, M. J., and F. Gibbs. 2000. Potential of earthworm burrows to transmit injected animal wastes to tile drains. *SSSA J.* 64(6): 2103-2109.
- Shipitalo, M. J., and F. Gibbs. 2005. Preferential flow of liquid manure in macropores and cracks. In *Proc. 2005 ASABE Annual International Meeting*. ASABE Paper No. 052063. St. Joseph, Mich.: ASABE.
- Shipitalo, M. J., V. Nuutinen, and K. R. Butt. 2004. Interaction of earthworm burrows and cracks in a clayey, subsurface-drained soil. *Appl. Soil Ecol.* 26(3): 209-217.

- Soller, J. A., M. E. Schoen, T. Bartrand, J. E. Ravenscroft, and N. J. Ashbolt. 2010. Estimated human health risk from exposure to recreational waters impacted by human and non-human sources of fecal contamination. *Water Res.* 44(16): 4674-469.
- Soupir, M. L., S. Mostaghimi, E. R. Yagow, C. Hagedorn, and D. H. Vaughan. 2006. Transport of fecal bacteria from poultry litter and cattle manures applied to pastureland. *Water Air Soil Pollut.* 169(1-4): 125-136.
- Sugg, Z. 2007. Assessing U.S. farm drainage: Can GIS lead to better estimates of subsurface drainage extent? Washington, D.C.: World Resources Institute. Available at: http://pdf.wri.org/assessing_farm_drainage.pdf. Accessed 16 May 2012.